Physical aging of polycarbonate far below the glass transition temperature: Evidence for the diffusion mechanism

D. Cangialosi,[1,3,*] M. Wübbenhorst,[1] J. Groenewold,[1,3] E. Mendes,[1] H. Schut,[2] A. van Veen,[2,†] and S. J. Picken[1,3]
[1]*Dept. of Polymer Materials and Engineering, Delft University of Technology, Julianalaan 136, 2628 BL, Delft, The Netherlands*
[2]*Interfaculty Reactor Institute, Delft University of Technology, Mekelweg 15, 2629 JB, Delft, The Netherlands*
[3]*Dutch Polymer Institute, P.O. Box 902, 5600 AX Eindhoven, The Netherlands*
(Received 11 May 2004; revised manuscript received 30 September 2004; published 30 December 2004)

Dielectric permittivity measurements and free volume determination by means of positron annihilation lifetime spectroscopy (PALS) were used to monitor physical aging of polycarbonate (PC) far below the glass transition temperature (Tg). The effect of film thickness and cooling rate from the melt was investigated to give new insight about the microscopic nature of the physical aging process. The results show that both the film thickness and the cooling rate play an important role in the kinetics of physical aging. A strong indication for a fully diffusive mechanism of physical aging is given, at least at the beginning of the aging process, where free volume holes disappear at a boundary which can either be the external surface of the sample or an internal surface defined by the presence of some low-density regions, which are created during the cooling process and have a concentration dependent on the cooling rate. In particular, the amount of internal surface is proportional to the cooling rate from the melt. Evidence for the existence of the low-density regions was provided by the absorption of ethylene glycol (EG), a molecule with a strong tendency to aggregate, in PC samples cooled down at different rates. The amount of absorbed EG was found to be proportional to the cooling rate. In addition, through dielectric spectroscopy in combination with thermogravimetric analysis, it was found that EG tends to locate in regions with large open space rather than in the bulk of PC. The physical origin for the formation of such regions might be related to the evolution of spatial heterogeneities during cooling from the supercooled state and its dependence on the cooling rate.

DOI: 10.1103/PhysRevB.70.224213 PACS number(s): 61.43.Fs, 61.20.Lc, 82.35.Lr, 78.70.Bj

I. INTRODUCTION

When a supercooled liquid is further cooled below the glass transition temperature, it falls out of equilibrium due to its reduced mobility. The achieved nonequilibrium state slowly evolves towards equilibrium, which consists of the recovery of the thermodynamics properties. This process is commonly regarded as physical aging or structural recovery and has been the subject of a large body of studies since the pioneering work of Simon,[1] Kovacs,[2] and Struik.[3] Several phenomenological models, which describe the kinetics of physical aging, were developed in the past.[3–5] The essential feature of these models is a distribution of sequentially activated relaxation processes, which is often described by a stretched exponential.[6] Still little is known, however, about the microscopic mechanisms of physical aging. In the early 1940's, Alfrey *et al.*[7] proposed that diffusion of free volume holes and their annihilation at the external surface of the sample could be responsible for the time evolution of the macroscopic thermodynamic properties. This hypothesis was later opposed by Braun and Kovacs,[2,8] who found a weak, if any, geometry dependence on the aging process. More recently, Curro *et al.*[9] successfully modeled the volume recovery of poly(vinyl acetate) (PVAc) through a diffusion mechanism. To explain the independence on sample geometry, they proposed an internal length scale for diffusion, which could be attributed to either an internal annihilation of vacancies or to a redistribution of free volume in an inhomogeneous glassy structure. In a similar way, Perez[10] modeled the physical aging of PVAc according to the migration and annihilation of defects of different sign corresponding to sites with positive and negative density fluctuations. In the last decade, several studies have been presented that document a sample thickness dependent aging process far below the glass transition temperature (T_g).[11–15] In particular, Pfromm *et al.* presented a number of studies on time-dependent gas transport properties. They provided evidence for an accelerated physical aging for thin films (around 1 μm) of polysulfone and a polyimide (6FDA-IPDA),[11] polynorborene,[12] and poly[1-(trimethylsilyl)-1-propyne] (PTSMP).[13] McCaig and Paul[14,15] reached similar conclusions following the time evolution of gas permeation properties for physical aging of thin films of a glassy polyarylate. Since the thickness dependence of physical aging disappears for thickness above several microns, they suggested that two mechanisms are responsible for physical aging: free volume diffusion to the film surface and lattice contraction.

In this study, the effect of sample geometry and thermal history is investigated to provide new insight about the role of free volume holes diffusion on the physical aging of polycarbonate (PC). In particular, apart from the film thickness, the role of the cooling rate from the equilibrium supercooled state (above T_g) is considered as a crucial parameter to determine the structural time evolution during physical aging. Two techniques are employed to probe the structural evolution: (i) the variation of the dielectric permittivity as a consequence of densification and (ii) the free volume evolution during physical aging as probed by means of positron annihilation lifetime spectroscopy (PALS). Very recently, this technique was successfully employed to study physical aging

of PC.[16,17] In particular, PALS allows a direct probing of the free volume sites in a polymer since the lifetime (τ_3) of *ortho*-positronium (*o*-Ps), the triplet state of the system electron-positron, is inversely proportional to the overlap of the positron component of the Ps wave function with the cavity wall electron wave function and is therefore related to the size of the low-electron density free-volume sites.[18] As will be seen below, the use of the two techniques mentioned above brought enough evidence that forced us to revisit the hypothesis of a diffusive process as the main mechanism for physical aging.

II. EXPERIMENTAL SECTION

A. Materials and sample preparation

Polycarbonate (PC) from General Electric (Lexan 161) was used for all the experiments. The glass transition temperature, measured using a Perkin-Elmer DSC-7 at a heating rate of 10 °C/min, was 147.5 °C. A large number of PC films in a thickness range between 6 and 800 μm were obtained for permittivity measurements. While films above 60 μm were obtained by compression molding at 100 °C above T_g, films below 60 μm were obtained by solution casting on a glass plate. The solvent used was dichloromethane and the solution concentration was adjusted to obtain the required film thickness. The 4 mm thick samples used for PALS measurements were all compression molded. All samples were dried in oven at 120 °C under vacuum for several days to remove moisture and/or any residual solvent. In order to remove the previous thermal history, all samples were heated up at 180 °C (about 30 °C above T_g) for several minutes and cooled down at four different cooling rates 0.02, 5, 60, and 100 °C/s.

B. Dielectric permittivity measurements

For accurate, long-term isothermal aging experiments, a custom-made dielectric spectrometer based on a Stanford Research DSP lock-in 830 in combination with a high-impedance dielectric interface was employed. Dielectric spectra were taken in the frequency range from 0.1 Hz to 30 kHz at an interval of 5 to 10 min in order to monitor the time evolution of the real part of the dielectric permittivity during physical aging. To study efficiently multiple samples over extended aging periods, we have employed a special sample cell containing four separate circular electrode systems. During the dielectric experiment, all samples were addressed sequentially by means of a coaxial multiplexer, a procedure which allowed the quasisimultaneous acquisition of four $C(t,f)$ data sets under practically identical conditions. The whole sample cell was kept in a glass Dewar, the temperature of which kept constant to 50 °C by an Eurotherm 808P temperature controller with an accuracy of ±0.1 K. All measurements were carried out in a nitrogen environment to avoid artifacts arising from the effect of time-dependent moisture uptake.

Since the measurement of extremely small capacity effects as the result of physical aging requires samples under well defined and reliable electrical and mechanical conditions, particular attention was paid to the sample metalization and mechanical fixation in the sample cell. All PC films were provided with a circular electrode of Au (20 mm in diameter) on both sides by a rf-sputter process. To ensure free expansion/contraction of the glassy samples, each film was sandwiched with a conducting "soft electrode" (Al wrapped silicon rubber, diameter 10–15 mm) and subsequently clamped between the rigid electrode system.

For temperature-dependent dielectric measurements, a broadband dielectric spectrometer based on a high precision dielectric analyzer (ALPHA, Novocontrol GmbH) and a Novocontrol Quatro cryosystem was used. Measurements were performed over a wide frequency (10^{-1}–10^7 Hz) and temperature range (−140–200 °C).

C. PALS measurements

PALS measurements were performed at room temperature on all the above mentioned samples, by exposing them to radioactive ^{22}NaCl with an activity of 10 μC sandwiched between two Kapton foils. As a rule, samples were aged at room temperature in vacuum in order to avoid any effect of time dependent moisture absorption on the PALS results, and collected only just before the PALS measurement. A fast-fast coincidence circuit of the PALS spectrometer at the IRI-TU Delft, with a lifetime resolution of 240 ps as monitored by using a ^{60}Co source, was used to record all PALS spectra. The spectrum is analyzed using the program POSITRONFIT, which describes the spectrum as a convolution of the instrument resolution function and a finite number of negative exponentials plus the background as described by the following equation:[19]

$$y(t) = R(t) \otimes \left(N \sum_{i=1}^{n} I_i \lambda_i \exp(-\lambda_i t) + B \right). \qquad (1)$$

Here $R(t)$ is the resolution function of the system, λ_i is the inverse of the annihilation time (annihilation rate), and B is the background signal. All spectra were resolved in three lifetime components: a short one of 125 ps related to *p*-Ps annihilation, an intermediate one of 400 ps related to free positron annihilation, and a long component ($\tau_{o\text{-Ps}}$) related to *o*-Ps annihilation.

A semiempirical relation was proposed to relate the lifetime of *o*-Ps to the size of the free volume site[20]

$$\tau_{o\text{-Ps}} = \frac{1}{2}\left[1 - \frac{R}{R+\Delta R} + \frac{1}{2\pi} \sin\left(\frac{2\pi R}{R+\Delta R} \right) \right]^{-1}, \qquad (2)$$

where R is the radius of the cavity and $\Delta R = 1.656$ Å is the electron layer thickness optimized for molecular solids.

In addition to the information on free volume hole size, a direct relation was proposed in the past between the intensity of *o*-Ps ($I_{o\text{-Ps}}$), namely, the probability of Ps formation and the free volume hole density.[21] Although the $I_{o\text{-Ps}}$ can be affected by a number of other factors, such as chemical composition of the polymer,[22] source strength and charging effects due to prolonged irradiation,[23–25] electric fields,[26,27] and visible light,[28] the proportionality between $I_{o\text{-Ps}}$ and the concentration of free volume holes can be still assumed, pro-

vided that all the mentioned effects are eliminated. This is the case of this study, where the chemical structure of PC does not change with time and the other factors affecting $I_{o\text{-Ps}}$ are not present. To avoid charging effects due to prolonged positron irradiation, the following precautions were taken: (i) only one sample is used for each measurement; and (ii) the number of counts collected for each sample was 2×10^6, which is low enough to avoid any significant charging during the measurement, as shown in our previous study where the same source was used.[25]

Unlike the permittivity measurements, in this case only the effect of cooling rate was tested. This is due to the fact that, since the ^{22}Na emits positrons with a distribution of energies, almost all of the positrons will be thermalized within the first millimeter of the sample. This means that samples above 1 mm will present the same response, while samples below 1 mm will suffer from the partial annihilation of positrons outside the sample, since the most energetic positrons will penetrate and escape the sample.

D. EG absorption

Several PC samples subjected to different cooling rates from the melt were immersed in anhydrous ethylene-glycol (EG) for three days. The EG uptake was measured and the so-obtained samples were used for dielectric spectroscopy and thermogravimetric analysis (TGA). Dielectric experiments were performed using a broadband dielectric spectrometer based on a high precision dielectric analyzer (ALPHA analyzer, Novocontrol GmbH) in combination with a Novocontrol Quatro temperature system providing control of the sample temperature with accuracy better than ±50 mK. Measurements were performed over a wide frequency range (10^{-1}–10^7 Hz). Temperature-dependent measurements were carried out isothermally in steps of 5 °C during heating from −140 to 190 °C. TGA analysis was performed with a Perkin Elmer TGA7 from 25 to 190 °C during heating and cooling. During the heating step, a heating rate that resembles the one of the dielectric measurements was used.

III. RESULTS

As already pointed out in the Introduction, physical aging is accompanied by the time evolution of the physical properties of the glass. Upon densification, the dielectric permittivity can show two opposing trends: (i) it increases due to the increased number of polarizable entities per unit volume or (ii) in the case of orientation polarization due to relaxed molecular dipoles, the permittivity decreases due to a reduced amplitude of angular fluctuations which usually establish the secondary relaxation processes in the glassy state.

One can show for our particular case of quasifreely contracting films, metalized with thin-film electrodes of variable area, that a density increase always causes an increase in the capacitance, provided that only fast (electronic and atomic) polarization processes contribute to the overall permittivity.[29] In view of the common observation for all aging experiments, that $C(t)$ exclusively reveal a decrease in the capacitance with time, we may conclude that the $C(t)$ response is governed by the second effect, the density related reduction in the relaxation strength of the secondary relaxations. This latter effect was shown in the past to be dominant during physical aging of amorphous PET and related polyesters.[30] In the present study, a similar trend was found and, therefore, the dielectric permittivity decreases with the aging time as a consequence of the densification of the system. This is shown in Fig. 1, where the normalized dielectric permittivity, namely, the ratio of the actual permittivity with the zero aging time permittivity, is plotted versus the aging time at 50 °C as a function of the film thickness and at constant cooling rate. In Fig. 2 the normalized dielectric permittivity relaxation is plotted at fixed thickness (800 μm as a function of the cooling rate. The zero aging time permittivity was obtained by plotting the absolute permittivity with the square root of the time and extrapolating at time zero by means of a linear fitting. The reason for this choice will become clear in the next section. All the figures refer to the permittivity measured at 12.8 Hz. However, no dependence on the frequency was found for all the investigated samples, up to 1 kHz. At higher frequencies the low-frequency tails of the α process probably shows up. Between 0.1 Hz and 1 kHz the real permittivity shows a flat signal that is normally observed between the α and β process. This is shown in the inset of Fig. 1(d), where, as an example, the permittivity-frequency plot is shown for a 16 μm sample cooled down at 100 °C/s for two different aging times This means that the permittivity reduction during physical aging can be fully attributed to a densification of the system and not to a relaxation shifting.

From the analysis of these figures, two crucial observations can be made. (i) The relaxation pattern is strongly dependent on the cooling rate as evidenced by comparing the relaxation strength at constant thickness (Fig. 2), although no differences are found for the two highest cooling rates (60 and 100 °C/s). (ii) The film thickness plays an important role in the physical aging of samples cooled down at 0.02 and 5 °C/s, while this effect, though present, is hardly visible for samples subjected to higher cooling rates. The influence of sample thickness on the physical aging was already revealed for films of the order of several microns or less.[11–15] However, to our best knowledge, the present results for the first time show a geometry-dependent physical aging process for "bulky" samples (of the order of few hundreds microns), although this dependence is very weak when the cooling rate before aging is increased above few degrees per second. On the other hand, the acceleration of physical aging with a cooling rate increase was already highlighted in several studies,[31–33] and rationalized in the framework of the Tool-Narayanaswamy-Moynhian[34] (TNM) and the Adams-Gibbs (AG) model.[35] From our results, it is clear that both the sample geometry and the cooling rate play a major role in influencing PC physical aging far below T_g.

This effect of cooling rate is also found from the PALS results. In our previous works on PC physical aging,[16,17] we have already detailed the microscopic nature of the free volume relaxation. In particular, we have shown that $\tau_{o\text{-Ps}}$, the lifetime of *o*-Ps, does not change during aging far below T_g, indicating a well-defined cavity size. In particular, a diameter of about 6 Å was found by means of Eq. (2). On the other

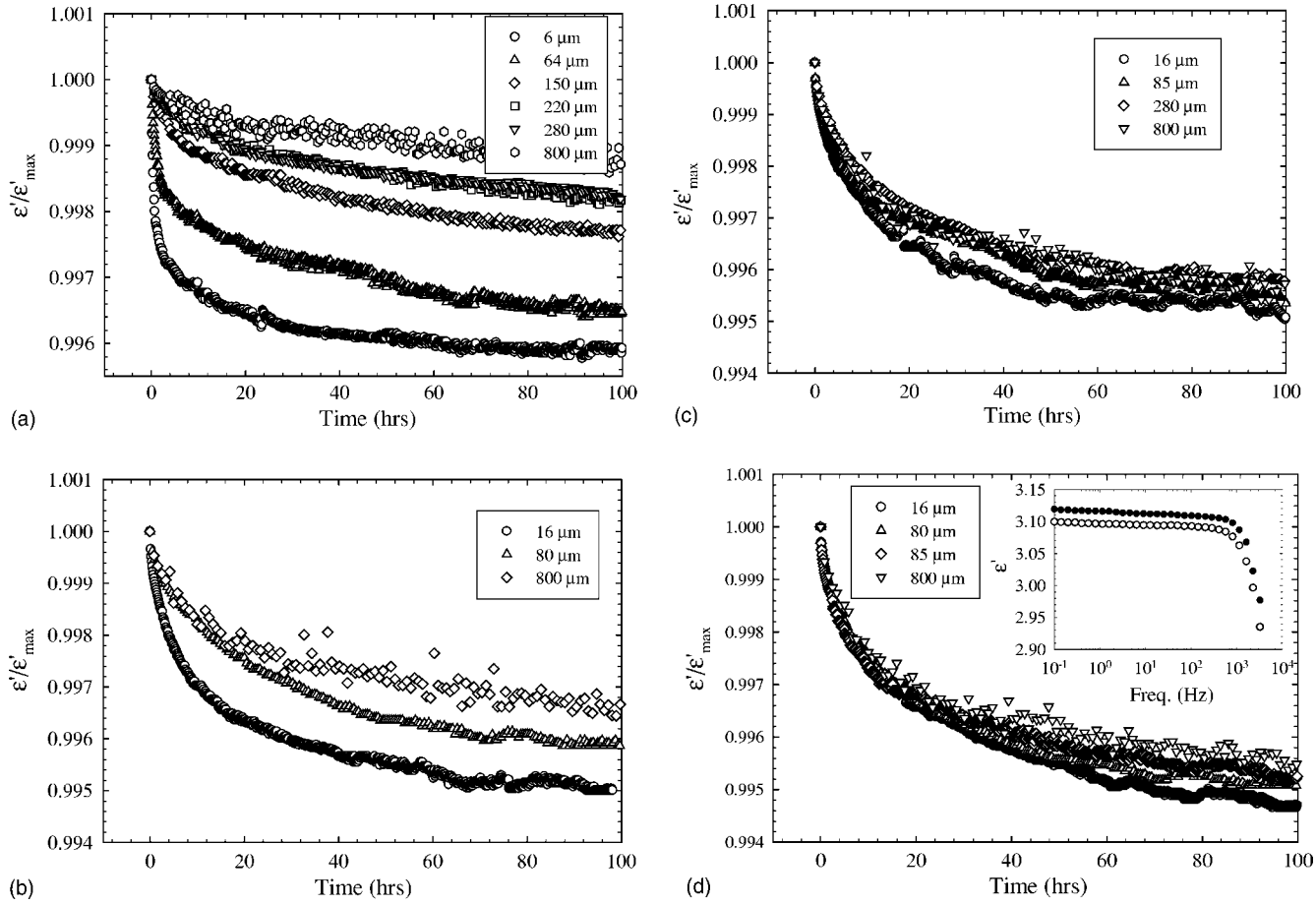

FIG. 1. Normalized permittivity at 12.8 Hz vs aging time at different thicknesses for the following cooling rates: (a) 0.02, (b) 5, (c) 60, and (d) 100 °C/s. See text for the definiton of the normalized permittivity. The inset of (d), which refers to a sample cooled down at 100 °C/s and with a thickness of 16 μm, shows the frequency sweep of the permittivity for zero aging time (filled circles) and for 100 h aging (empty circles).

hand, $I_{o\text{-Ps}}$ the intensity of *o*-Ps, clearly decreases with the aging time, meaning that somehow the concentration of free volume holes in the system gradually decreases. Similar results were obtained in this study and they are summarized in Fig. 3, where the decrease of $I_{o\text{-Ps}}$ with aging at four different cooling rates is shown.

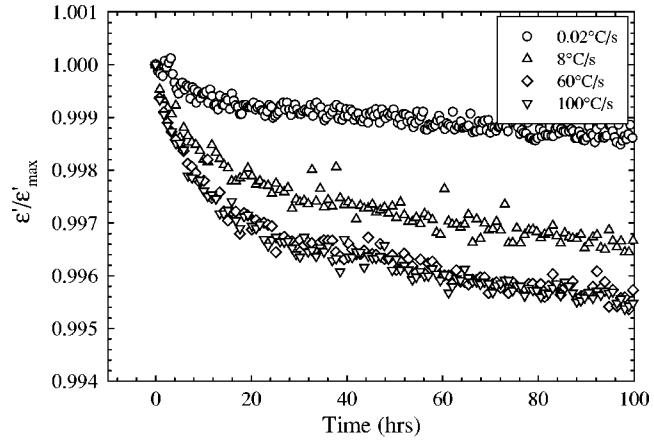

FIG. 2. Normalized permittivity at 12.8 Hz vs aging time for a fixed thickness of 800 μm at each cooling rate.

By comparing the figures, we observe that the cooling rate dependence of the free volume relaxation resembles the permittivity relaxation shown in Fig. 2, i.e., the higher the cooling rate the faster the physical aging of the system. It is worth noticing that the permittivity relaxation occurs faster than the free volume relaxation. However, this difference can be explained if one takes into account that PALS experiments are carried out at 25 °C, while the permittivity relaxation is measured at 50 °C. Therefore, since physical aging is temperature dependent, the temperature difference can explain difference in the time scale.

Another important observation results from extrapolating the $I_{o\text{-Ps}}$ to zero aging time. The extrapolation was carried out as previously described for the dielectric permittivity. The so-obtained initial values of the $I_{o\text{-Ps}}$ are summarized in Table I. It is interesting to notice that the lower the cooling rate the higher $I_{o\text{-Ps}}$ at the beginning of the aging process becomes. This result is in contradiction with the fact that at low cooling rate a low T_g has to be expected, which, in turn, would lead to a denser glass and, therefore, to a lower concentration

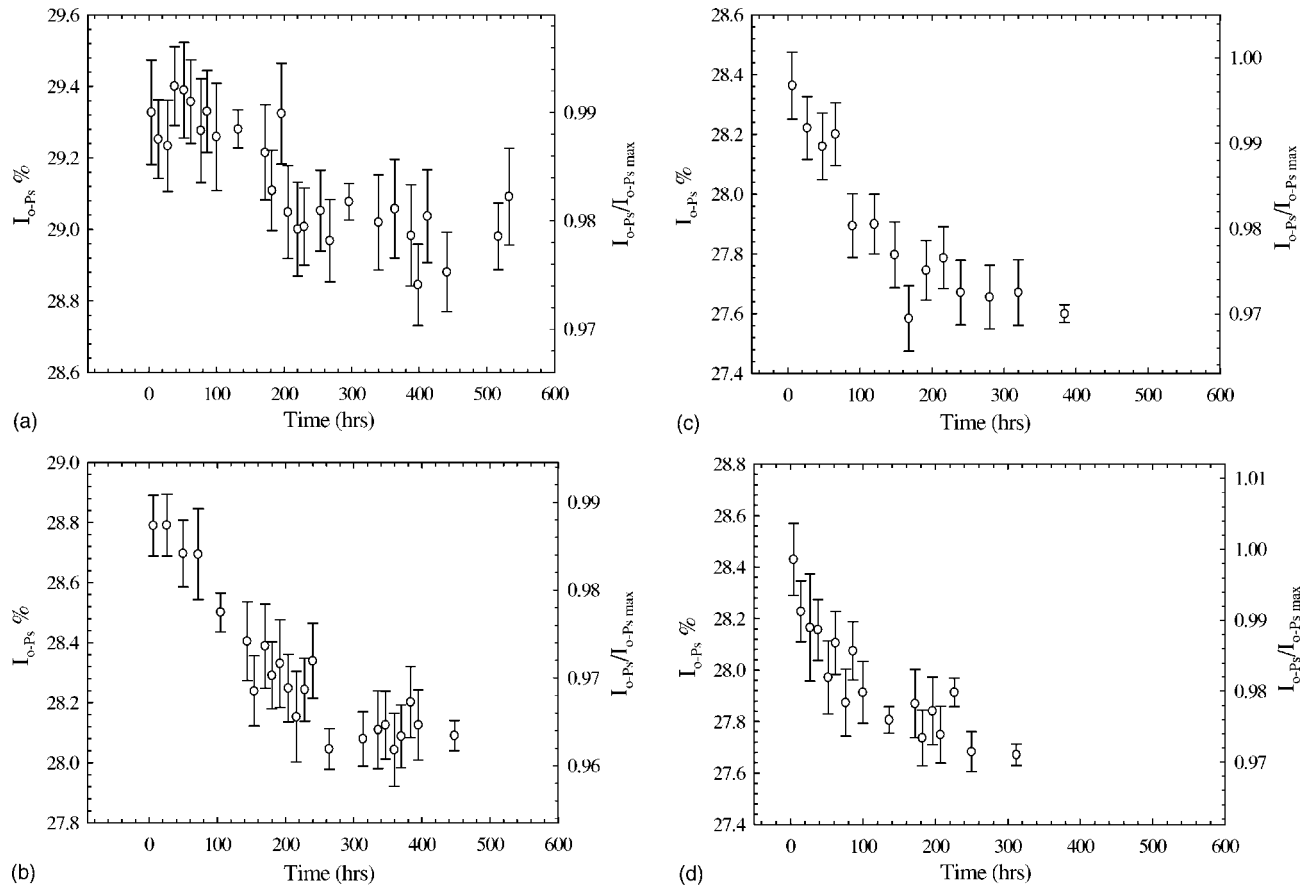

FIG. 3. $I_{o\text{-Ps}}$ (left axis) and normalized $I_{o\text{-Ps}}$ (left axis) vs aging time for 4 mm thick samples for the following cooling rate: (a) 0.02, (b) 5, (c) 60, and (d) 100 °C/s. See text for the definition of the normalized $I_{o\text{-Ps}}$.

of holes. An explanation for this unexpected behavior will be provided in the discussion.

Finally, $I_{o\text{-Ps}}$ during physical aging was normalized by making use of the initial values from Table I. This is shown in the right axis of Figs. 3(a)–3(d).

IV. DISCUSSION

From a microstructural point of view, physical aging can be described as a process that produces a reduction in the free volume. To simplify the discussion we will consider the glass as a lattice, where the bulk is represented by the occupied lattice sites and the free volume fraction by the empty lattice sites. In general, to achieve a free volume reduction, two mechanisms in principle are possible: (i) lattice contraction and (ii) reduction of the number of lattice sites. From a PALS point of view, the first mechanism would produce a reduction in $\tau_{o\text{-Ps}}$, i.e., the cavity size, while the second mechanism leads to a reduction in $I_{o\text{-Ps}}$, i.e., a reduction in the concentration of free volume holes. An excellent example of the first process is densification of amorphous polymers in the melt state via the application of isostatic pressure, which actually leads to a reduction in $\tau_{o\text{-Ps}}$.[36] In the case of physical aging of PC, the mechanism of densification follows the second mechanism, since, as noted in the previous section of the paper, the free volume relaxation occurs via a reduction in the $I_{o\text{-Ps}}$. The reduction of the hole concentration, i.e., the number of empty lattice sites, is compatible with the hypothesis of a diffusion mechanism which drives the physical aging process. If we identify the length scale for diffusion with the macroscopic dimensions of the sample, we have a clear indication of the effect of thickness for PC samples cooled down at 0.02 and 5 °C/s as shown in Figs. 1(a) and 1(b). However, for samples cooled down at higher rates the influence of the dimensions of the sample, although present, is weak. As discussed in the Introduction, previous studies provide evidence for a thickness dependence of physical aging for relatively high cooling rates,[11–15] where this dependence appears at a thickness of about 1 μm or less. McCaig *et al.*[14,15] attempted to explain these experimental facts by hypothesizing that physical aging occurs through a double

TABLE I. Summary of experimental and fitted parameters from permittivity and PALS measurements at different cooling rates.

Cooling rate (°C/s)	$I_{o\text{-Ps max}}$	Absorbed EG (vol. %)	D (cm^2/s)	A_{int}/V ($1/\mu$m)
0.02	29.612	0.025	1.73×10^{-15}	4.85×10^{-3}
5	29.154	0.065	3.06×10^{-16}	4.22×10^{-2}
60	28.448	0.194	3.75×10^{-17}	1.63×10^{-1}
100	28.454	0.198	3.54×10^{-17}	1.85×10^{-1}

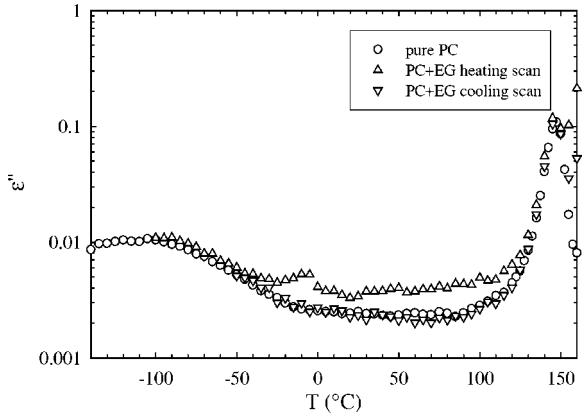

FIG. 4. Dielectric loss vs temperature at 1.2 Hz for pure PC and PC-EG systems during heating and cooling.

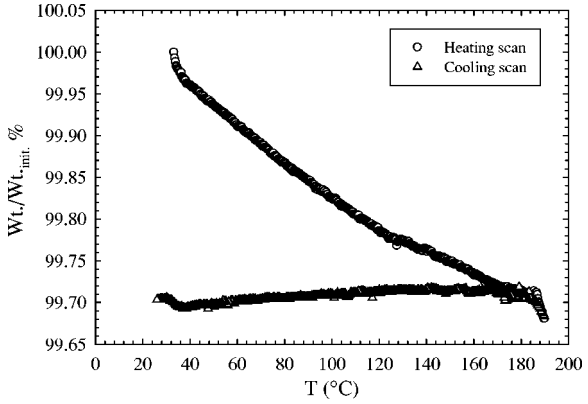

FIG. 5. TGA analysis for PC-EG system during heating and cooling.

mechanism: lattice contraction and diffusion of free volume holes.

However, since the cavity size remains constant, as shown by PALS, we can exclude the former mechanism as the driving force for physical aging. We believe that the present results provide evidence for a fully diffusive mechanism to be responsible for physical aging. To explain this, we will assume that not only the external surface is responsible for disappearance of free volume cavities, but that also an internal surface, which is somehow created during cooling from the supercooled state, contributes to this process. In other words, we are assuming that the inhomogeneity of the glass gives rise to low-density regions that act as an internal surface for vacancies annihilation. To demonstrate the existence of such an internal surface, a number of PC samples subjected to the same cooling rates used for aging experiments were exposed to ethylene glycol (EG) for a fixed time of three days. EG was chosen for its high tendency to aggregate in low density regions, as recently demonstrated by Smits *et al.* for a starch polysaccharide.[37] After this treatment, the PC samples were weighed in order to evaluate the amount of absorbed EG. The results are summarized in Table I, where the percentage of absorbed EG is shown for each cooling rate. A clear dependence on the amount of absorbed EG can be observed. In particular, a positive correlation exists between the amount of absorbed EG and the cooling rate. For the two highest cooling rates (60 and 100 °C/s) not much difference is observed. To provide more detailed information on the underlying structure, dielectric spectroscopy combined with TGA was employed. Figure 4 shows the isochronal dielectric loss at 1.2 Hz of the EG-saturated PC over a wide temperature range, both in heating and subsequent cooling, together with the data of pure (dry) PC. Though Fig. 4 refers to PC samples subjected to a cooling rate of 60 °C/s, a qualitatively similar behavior was found also for the other cooling rates.

These results can be summarized as follows. (i) Both the α and β process of PC remain substantially unaltered in the presence of EG (the high loss above T_g for the system PC-EG is due to a high conductive contribution). (ii) During the heating scan the presence of EG generates a broad loss between the α process of PC and α process of EG (located at −80 °C at about 1 Hz). (iii) This broad loss vanishes in the subsequent cooling scan. These findings indicate that, rather than being homogeneously distributed in the "bulk" of PC, EG tends to be concentrated in low-density regions of the PC, giving rise to a T_g in-between that of PC and EG. In fact, a homogeneous distribution of EG can be excluded since, in this case, PC α process would experience a change in the dynamics. Neither the dielectric response can be attributed to some EG located in the outer surface of the sample because this would rise to the α process of EG.

The TGA data, shown in Fig. 5, are in agreement with the former conclusion. As we can see in this figure, EG gradually evaporates during the heating scan and is absent during the cooling scan. However, a considerable amount of EG is still present during the heating scan in the neighborhood of the T_g of PC. Combining this observation with the fact that the α process of PC is unaltered by the presence of EG reinforces the idea the EG locates in some low-density regions, which are created during the cooling step from the melt.

Moreover, the presence of these low-density regions may provide an explanation of the observation that the $I_{o\text{-Ps}}$ decreases with increasing the cooling rate. It is important to note that the *o*-Ps fraction that annihilates in these low-density regions most likely will not be collected by our fast-fast coincidence circuit for two reasons: (i) the acquisition time window is not wide enough to acquire annihilation events with a lifetime longer than several nanoseconds, which is probably the case in low density regions, (ii) the annihilation in these regions probably occurs via three γ annihilation,[38] and the energy window of our system is not set to acquire these events. Therefore, if we take into account the free volume directly probed by PALS and the free volume confined in the low density regions, which increases with the cooling rate, we can reconcile, at least qualitatively, the observation of a decreasing $I_{o\text{-Ps}}$ with the cooling rate, with thermodynamic and kinetic considerations, which indicate an overall free volume proportional to the cooling rate. In other words, the free volume can be schematically classified in two parts: the one directly probed by PALS, which is representative of the denser regions; and the one, not probed by PALS, representative of less dense regions. This classification arises from the heterogeneous nature of the glassy

state[39] and its cooling rate-dependent evolution from the supercooled state.[40–42] The results of the EG absorption and PALS experiments are in agreement with molecular dynamics simulations on a binary Lennard-Jones mixture[40,41] and on amorphous silica[42] cooled down from the supercooled state at different rates. These simulations reveal that, with decreasing cooling rate the system achieves increasing local order, which causes a smaller number of low-density regions to form in the glass.

As we have demonstrated the presence of some low-density regions which are somewhat distinguished from the bulk PC, we can analyze our data according to a diffusion model, where the boundary surface for free volume holes disappearance can be either the external surface and the internal surface created by the low-density regions. In particular, we have considered the rate of free volume holes disappearance at zero aging time, when the amount of free volume is still at its initial value all over the bulk PC. The diffusion of free volume can be expressed by the second equation of Fick

$$\frac{\partial f_v}{\partial t} = \nabla (D \nabla f_v), \tag{3}$$

where f_v is the free volume fraction and D is the diffusion coefficient. If we develop Eq. (3) around $t=0$, we can assume a constant D, since the well-known effect of self-retardation[3] has not yet provoked a substantial decrease of D. Within our simplified picture the total number of free volume holes at time t, $N(t)$, equals the integral over the sample volume of the f_v over the cavity volume, which is constant during physical aging. Note that $N(t)$ is proportional to $I_{o\text{-Ps}}$ in the PALS measurements. With the diffusion Eq. (3), the following expression for $N(t)$ can be obtained for short aging times:

$$\frac{N(t)}{N(0)} = 1 - \frac{2}{\pi^{0.5}} \frac{A}{V} D^{0.5} t^{0.5}, \tag{4}$$

where A is the total surface where free volume holes disappear, V is the total volume, D is the diffusion coefficient at zero aging time, t is the aging time, and $N(0)$ is the number of holes at zero aging time. Equation (4) is arrived at by considering the free volume flux of the diffusing holes by simple Fickian diffusion through a planar surface near $t=0$. If we multiply this flux, which equals $N(0)(D/\pi t)^{0.5}$, with the total area of absorbing surface A, we get the rate of the total number of holes $N(t)$. Then by integration we arrive at Eq. (4). The replacement of the unknown distribution of absorbing surface by a half space problem is justified as long as the depletion layer of the disappearing free volume is smaller than the radius of curvature of the absorbing surface or the distance between surfaces, i.e., as long as the timescales are short enough. The behavior at long times requires a more detailed analysis and is expected to approach to equilibrium asymptotically.

It is very interesting to notice that from a mathematical point of view, Eq. (4) is equivalent to the stretched exponential of the Kohlrausch-Williams-Watt (KWW) model.[6] In fact, if the stretched exponential is expanded through a Taylor series around zero aging time, an expression analogous to Eq. (4) is obtained, provided that the stretched exponent equals 0.5. Values between 0.2 and 0.8 are usually found in literature without constraints in the fitting.[34] In this case, a totally different physical interpretation is given: while the KWW was explained with the hypothesis of a distribution of relaxation times, in this case an equivalent mathematical form arises from the hypothesis of a diffusion model. According to this model, the KWW relaxation time can be expressed in terms of the diffusion coefficient and the ratio internal area/volume in the following manner: $\tau_{\mathrm{KWW}} \propto D^{-1}(V/A)^2$.

Equation (4) can be differentiated with respect to the square root of the time at $t=0$:

$$\left.\frac{d[N(t)/N(0)]}{d(t^{0.5})}\right|_{t=0} = -\frac{2}{\pi^{0.5}} \frac{A}{V} D^{0.5}. \tag{5}$$

This equation can be applied to our time-dependent permittivity data, if we make the reasonable assumption that the variation of the free volume produces a linearly proportional variation in the permittivity, at least in the vicinity of $t=0$. Therefore, Eq. (5) can be written in terms of the dielectric permittivity

$$\left.\frac{d[\varepsilon'(t)/\varepsilon'(0)]}{d(t^{0.5})}\right|_{t=0} = -\frac{2}{\pi^{0.5}} \frac{A}{V} D^{0.5}. \tag{6}$$

The surface A can be divided in two contributions: the external surface A_{ext}, related to the macroscopic dimensions of the sample, and the internal surface A_{int}, which is the boundary between the bulk PC and the low-density regions. The external surface can be expressed in terms of the sample thickness s and sample volume V: $A_{\mathrm{ext}}=V/s$. In this way, Eq. (6) becomes

$$\left.\frac{d[\varepsilon'(t)/\varepsilon'(0)]}{d(t^{0.5})}\right|_{t=0} = -\frac{2}{\pi^{0.5}} \left(\frac{1}{s} + \frac{A_{\mathrm{int}}}{V}\right) D^{0.5}, \tag{7}$$

where s is the thickness of the sample.

Equation (7) suggests that if we take the derivative of the normalized permittivity with the square root of the time at zero aging time $\{d[\varepsilon'(t)/\varepsilon'(0)]/d(t^{0.5})|_{t=0}\}$, at different thickness and constant cooling rate, which means fixed A_{int}, and plot it versus the inverse film thickness, it is possible to obtain information on both the ratio internal surface/volume and the diffusion coefficient at the beginning of the aging process. This is shown in Figs. 6(a)–6(d) for each cooling rate.

From the results in this figure, we conclude that a linear proportionality between $d[\varepsilon'(t)/\varepsilon'(0)]/d(t^{0.5})|_{t=0}$ and the inverse thickness holds for all cooling rates, as envisaged by Eq. (7). Only $d[\varepsilon'(t)/\varepsilon'(0)]/d(t^{0.5})|_{t=0}$ related to a thickness of 6 μm for a cooling rate of 0.02 °C/s [see inset of Fig. 6(a)] deviates from the linear fitting. In particular, it appears to be underestimated with respect to the linear fitting. However, for such a low thickness the hypothesis that the internal surface depends only on the cooling rate could be wrong. In fact, this low thickness can interfere with the formation of the low-density regions, if the distance between these regions approaches the macroscopic dimensions of the sample. This is particularly crucial for the lowest cooling rate, which gives

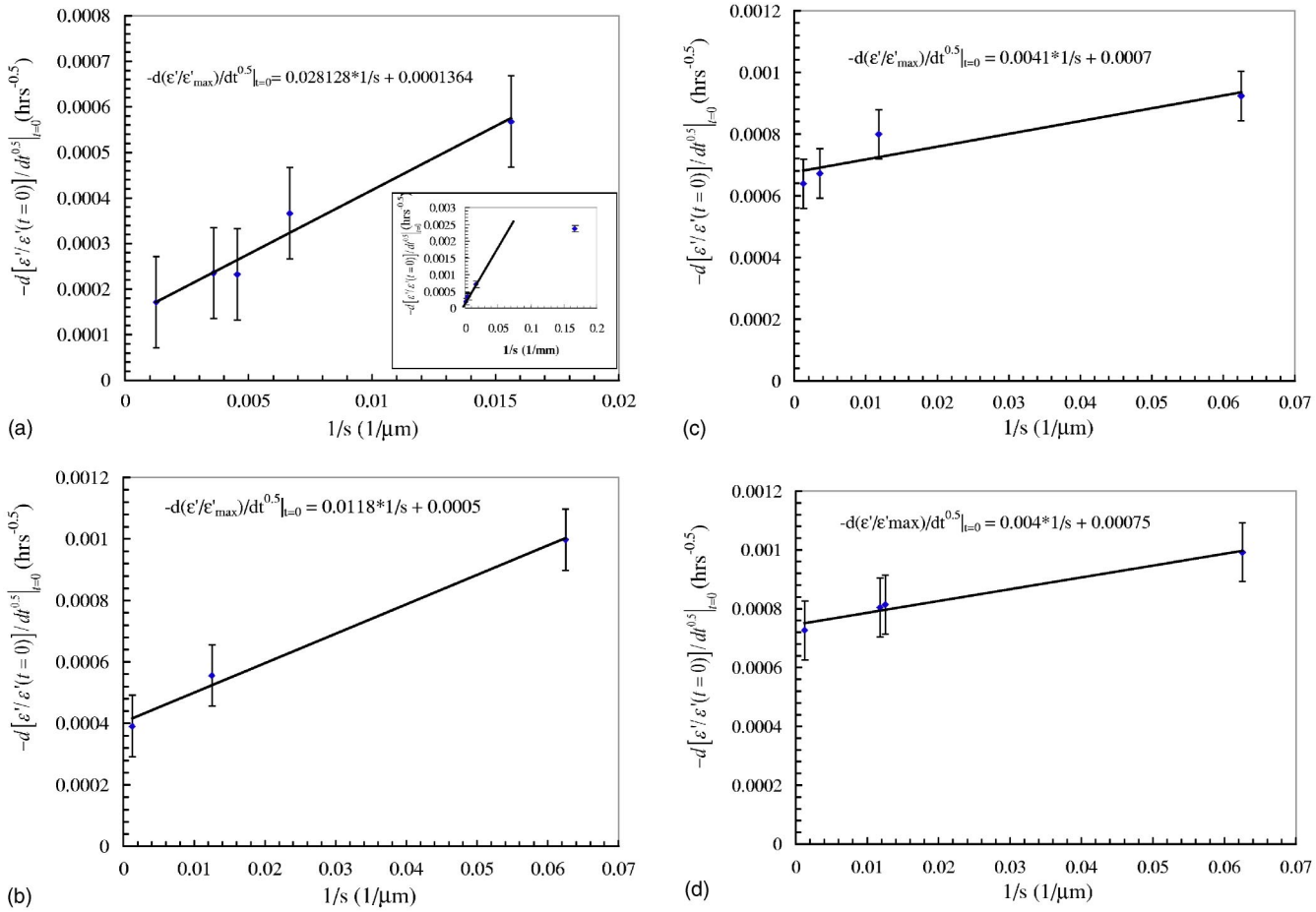

FIG. 6. Derivative of the normalized permittivity with the square root of the time vs the inverse of the sample thickness for the following cooling rates: (a) 0.02 °C/s (the inset includes also a thickness of 6 μm), (b) 5, (c) 60, and (d) 100 °C/s. The solid lines represent the linear fitting of the data points. The fitted equations are also shown in the figure.

rise to the largest distance between low-density regions. The results of the linear fitting of the data in Fig. 6 are summarized in Table I, where the diffusion coefficient and the ratio internal surface/volume are reported for each cooling rate. As expected, the ratio internal surface/volume increases with the cooling rate.

By comparing the diffusion coefficients obtained at different cooling rates, a clear decrease with the cooling rate can be observed. The diffusion coefficients at different cooling rates can be compared with the free volume as probed by PALS. In fact, it is well known that these two properties are related, since the early work of Doolittle.[43] In particular, the diffusion coefficient is related to the amount of free volume through the Doolittle equation

$$\ln D = \ln D_0 + \frac{B}{f_{v0}} - \frac{B}{f_v}, \tag{8}$$

where B is a material constant and f_{v0} is the reference free volume with diffusion coefficient D_0. Since only $I_{o\text{-Ps}}$ depends on the cooling rate and not $\tau_{o\text{-Ps}}$, we can write Eq. (8) in terms of $I_{o\text{-Ps}}$:

$$\ln D = \ln D_0 + \frac{B'}{I_{o\text{-Ps},0}} - \frac{B'}{I_{o\text{-Ps}}}. \tag{9}$$

If we plot $\ln D$ versus the inverse of $I_{o\text{-Ps}}$, a linear relation has to be obtained to prove the validity of the diffusion

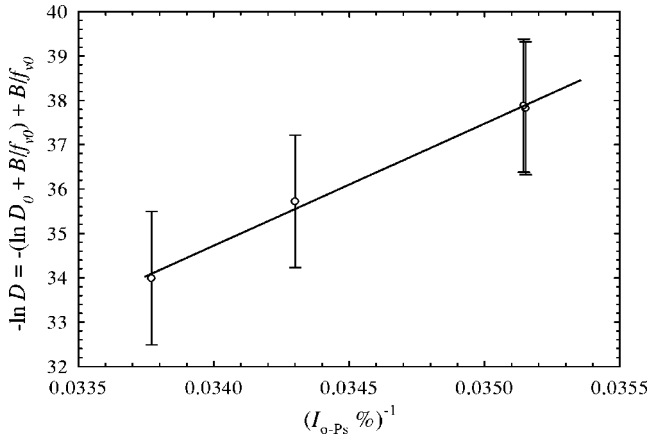

FIG. 7. Natural logarithm of the diffusion coefficient, proportional to the inverse of the free volume according to the Doolittle equation vs the inverse of the $I_{o\text{-Ps}}$.

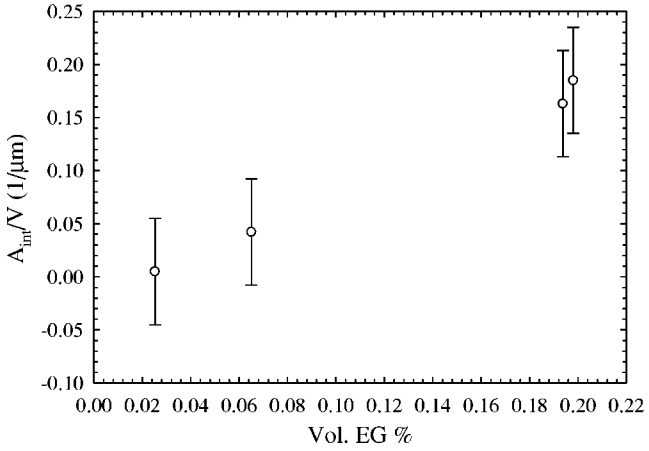

FIG. 8. Volume percentage of absorbed EG vs ratio internal area/volume as obtained from the fitting of the permittivity relaxation data. Each data point corresponds to each cooling rate.

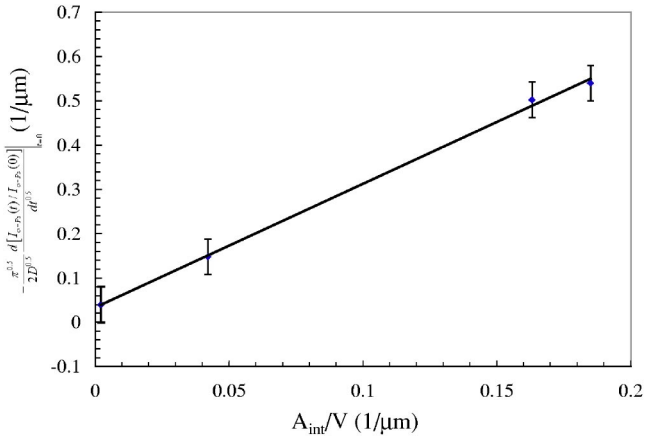

FIG. 9. First term of Eq. (10) vs the ratio internal area/volume as determined by fitting the permittivity relaxation data.

mechanism for physical aging. This is shown in Fig. 7 where, in agreement with our expectations, a linear relationship is found within the experimental error. This means that the comparison between parameters obtained from two different techniques seems to validate the diffusion mechanism for physical aging.

These results also suggest that the effect of acceleration of physical aging that occurs after fast cooling is not due to the larger amount of free volume present but to the highly inhomogeneous nature of the obtained glass. The effect of self-retardation that slows down physical aging at large times,[3] is not denied by these results, although a different interpretation is given for the fast physical aging of samples cooled down at high cooling rates. Here, we suggest that acceleration of physical aging is due to the presence of a large amount of internal surface, related to the inhomogeneity of the glass, which acts as a sink for the disappearance of free volume holes. Moreover, the increase of the diffusion coefficient of the free volume holes with decreasing cooling rate, although counterintuitive, is in agreement with a recent study on the effect of cooling rate on the gas transport properties in PC.[33] Also in this case, an increase of the diffusion coefficient of gas molecules is observed with decreasing the cooling rate, although the explanation provided in this work is different from ours.

The values of the ratio internal surface/volume, obtained from the analysis of the permittivity data, can be compared with the amount of EG absorbed in the PC at different cooling rates. If the hypothesis of a diffusion mechanism holds, provided that both the macroscopic dimensions of the sample and an internal surface created by the presence of the low-density regions are taken into account, there should be a positive correlation between absorbed EG and internal surface. This correlation is shown in Table I and also in Fig. 8, in which the ratio internal surface/volume is plotted versus the volume of absorbed EG. One more time, an indication for a fully diffusion driven physical aging is given. Note that at zero internal surface a residual amount of EG can be absorbed in PC, likely due to the ability of EG to create its own space, even in internal surface free sample.

In a similar manner, it is possible to analyze the PALS results. In this case, Eq. (5) can be expressed in terms of $I_{o\text{-Ps}}$ relaxation, since the free volume variation can be fully attributed to a decrease in the concentration of free volume holes [$N(t)$ is proportional to $I_{o\text{-Ps}}(t)$, as previously discussed]. The following equation can therefore be written:

$$-\frac{\pi^{0.5}}{2D^{0.5}}\frac{d[I_{o\text{-Ps}}(t)/I_{o\text{-Ps}}(0)]}{d(t^{0.5})}\bigg|_{t=0}=\frac{1}{s}+\frac{A_{\text{int}}}{V}. \qquad (10)$$

This equation again makes a distinction between the macroscopic dimensions of the system and the internal surface as in Eq. (7).

If we plot the experimental values of the normalized $I_{o\text{-Ps}}$ [Figs. 3(a)–3(d)] with the square root of the time, we can obtain the term $d[I_{o\text{-Ps}}(t)/I_{o\text{-Ps}}(0)]/d(t^{0.5})|_{t=0}$ for every cooling rate. Since each cooling rate corresponds to a fixed internal surface and the PALS experiments were done at fixed thickness, it is possible to plot the first term of Eq. (10) with the ratio internal surface/volume as obtained from the previous analysis on the permittivity relaxation data. Also the diffusion coefficients at each cooling rate were taken from the fitted permittivity data. This is shown in Fig. 9 where a linear relationship can be observed, in agreement with the diffusion model. The slope of the straight line larger than one, as would be required by Eq. (10), can be explained with the fact that we are using diffusion coefficients from permittivity relaxation at 50 °C, while the PALS data are obtained at 25 °C; and/or with the ability of PALS to probe free volume holes only in a certain size range.

The linear fitting of Fig. 9 also allows the calculation of a typical macroscopic dimension of the sample. The value found was 54 μm. This seems to be far too small compared to the real dimension of the samples used for PALS, which have a thickness of 4 mm. However, one has to consider that positrons are thermalized within the first millimeter of the PC sample. In addition, the positron implantation profile is well described by an exponential law,[38] which means that thermalized positrons are strongly concentrated in the first hundred microns of the sample. This gives a reasonable explanation to the value obtained from our fitting procedure.

However, for the same reason that we cannot obtain a slope of one from the linear fitting, the value of the macroscopic dimension of the sample can be somewhat different from the obtained one.

As we have provided evidences for a diffusion model for physical aging of PC, it is worth comparing our permittivity and free volume relaxation data with the volume relaxation data already reported in the literature.[44,45] In these studies, no specific volume reduction is observed for PC volume relaxation at 25 °C in the time scale of several days, which is the time scale for both permittivity and free volume relaxation. This is compatible with the idea of diffusion towards some internal surface. In fact, at least at the beginning of the physical aging process, the free volume released from the bulk will make the previously defined low-density regions even less dense. Since the specific volume measurement does not discriminate between the bulk and the low-density regions, no overall volume change will be observed at the beginning of the aging process. On the other hand, stress relaxation experiments during physical aging of PC far below T_g,[46] which is probably more sensitive to the structural changes in the bulk of the glass and less sensitive to the low-density regions, show relaxation effects already in the time scale of several days, in agreement with our permittivity and PALS results.

In conclusion, it is worth remarking that PC physical aging was fitted through a diffusion model for relaxation data obtained far below T_g, where the system is deeply in the glassy state and secondary relaxation processes are likely to have a dominant role in influencing the physical aging process, as demonstrated by some of us in a previous study.[17] On the other hand, physical aging just below the T_g is dominated by the cooperative motion responsible for the α process. In this case the glassy system possesses enough mobility that the static scenario based on more or less dense regions cannot be drawn and, therefore, physical aging more likely occurs via a long-range reorganization.

V. CONCLUSIONS

We have studied the physical aging of polycarbonate (PC) far below T_g by monitoring the time evolution of the permittivity and the free volume as probed by means of positron annihilation lifetime spectroscopy (PALS). The effect of film thickness and cooling rate was investigated. The permittivity was found to decrease during physical aging, due to the decreased mobility as a consequence of densification, which results in a smaller amplitude of dipole orientation and/or in a decreased number of dipoles able to reorient. The $I_{o\text{-Ps}}$, related to the concentration of free volume holes, was found to decrease with aging time, while the $\tau_{o\text{-Ps}}$, related to the cavity size, remains constant during physical aging. The decrease of the concentration of free volume holes is compatible with a diffusion mechanism for physical aging. Therefore, permittivity and PALS relaxation data were fitted according to a diffusion model around zero aging time, namely, when the concentration of free volume is at its initial value and the effect of self-retardation has not yet appeared. The outcome was that a diffusion model accurately describes the experimental results, when an internal surface was assumed to be present. Such an assumption is needed in order to overcome the inability of the macroscopic dimensions of the sample to fulfil the requirements of a diffusion model. The internal surface was related to the presence of some low-density regions. Evidence for the existence of such regions was given by absorbing ethylene glycol (EG), a molecule with a strong tendency to aggregate, in the PC samples and measuring EG uptake at different cooling rates together with the dielectric and a thermo-gravimetric results. Assuming the presence of low-density regions gives good agreement between the experiments and the diffusion model. The physical origin of the low-density regions and the dependence on the cooling rate may be related to the evolution of spatial heterogeneities during the cooling process.

ACKNOWLEDGMENTS

The work of D. Cangialosi, J. Groenewold, and S. J. Picken forms part of the research program of the Dutch Polymer Institute (DPI). This work is carried out under DPI Project No. 285: "Influence of Applied Stress and Physical Ageing on Diffusion and Solubility of Oxygen and Anti-Oxidants."

*Present address: Fundacion Donostia International Physics Center, Paseo Manuel de Lardizabal, 4-20018 San Sebastian, Spain.
†Deceased.

[1] F. Simon, Z. Anorg. Allg. Chem. **203**, 219 (1931).
[2] A. J. Kovacs, Adv. Polym. Sci. **3**, 394 (1963).
[3] L. C. E. Struik, *Physical Aging in Amorphous Glassy Polymers and Other Materials* (Elsevier Science, Amsterdam, 1978).
[4] A. Q. Tool, J. Am. Ceram. Soc. **29**, 240 (1946); O. S. Narayanaswamy, *ibid.* **54**, 491 (1971).
[5] A. J. Kovacs, J. J. Aklonis, J. M. Hutchinson, and A. R. Ramos, J. Polym. Sci., Polym. Phys. Ed. **17**, 1097 (1979).
[6] R. Kohlrausch, Ann. Phys. (Leipzig) **91**, 56 (1854).
[7] T. Alfrey, G. Goldfinger, and H. Mark, J. Appl. Phys. **14**, 700 (1943).
[8] A. J. Kovacs, J. Polym. Sci. **30**, 131 (1958).
[9] J. G. Curro, R. R. Lagasse, and R. Simha, Macromolecules **15**, 1621 (1982).
[10] J. Perez, Polymer **29**, 483 (1987).
[11] P. H. Pfromm and W. J. Koros, Polymer **36**, 2379 (1995).
[12] K. D. Dorkenoo and P. H. Pfromm, J. Polym. Sci., Polym. Phys. Ed. **37**, 2239 (1999).
[13] K. D. Dorkenoo and P. H. Pfromm, Macromolecules **33**, 3747 (2000).
[14] M. S. McCaig and D. R. Paul, Polymer **41**, 629 (2000).
[15] M. S. McCaig, D. R. Paul, and J. W. Barlow, Polymer **41**, 639 (2000).

[16] D. Cangialosi, H. Schut, A. van Veen, and S. J. Picken, Macromolecules **36**, 142 (2003).
[17] D. Cangialosi, M. Wübbenhorst, H. Schut, A. van Veen, and S. J. Picken, Phys. Rev. B **69**, 134206 (2004).
[18] W. Brandt, S. Berko, and W. W. Walker, Phys. Rev. **120**, 1289 (1960).
[19] P. Kirkegaard, M. Eldrup, O. E. Mogensen, and N. J. Pedersen, Comput. Phys. Commun. **23**, 307 (1981).
[20] M. Eldrup, D. Lightbody, and J. N. Sherwood, Chem. Phys. **63**, 51 (1981).
[21] V. P. Shantarovich, J. Radioanal. Nucl. Chem. **210**, 357 (1996).
[22] C. Wastlund and F. H. J. Maurer, Polymer **39**, 2897 (1998).
[23] M. Welander and F. H. J. Maurer, Mater. Sci. Forum **105–110**, 1811 (1992).
[24] X. S. Li and M. C. Boyce, J. Polym. Sci., Polym. Phys. Ed. **31**, 869 (1993).
[25] D. Cangialosi, H. Schut, M. Wübbenhorst, J. van Turnhout, and A. van Veen, Radiat. Phys. Chem. **68**, 507 (2003).
[26] C. L. Wang, K. Hirata, J. Kawahara, and Y. Kobayashi, Phys. Rev. B **58**, 14 864 (1998).
[27] A. Alba García, L. D. A. Siebbeles, H. Schut, and A. van Veen, Radiat. Phys. Chem. **68**, 515 (2003).
[28] J. Zrubcova, J. Kristiak, W. B. Pedersen, N. J. Pedersen, and M. Eldrup, Mater. Sci. Forum **363**, 359 (2001).
[29] We have to realize that in our experiments, primary the capacitance is measured, a quantity which is related to the permittivity by the simple expression $C=\varepsilon_0\varepsilon A/s$ and thus is also susceptible to dimensional changes.
[30] E. A. McGonigle, J. H. Daly, S. D. Jenkins, J. J. Liggat, and R. A. Pethrick, Macromolecules **33**, 480 (2000).
[31] H. C. Booij and J. H. M. Palmen, Polym. Eng. Sci. **18**, 781 (1978).
[32] I. M. Hodge and A. R. Berens, Macromolecules **15**, 756 (1982).
[33] C. M. Laot, E. Marand, B. Schmittmann, and R. K. P. Zia, Macromolecules **36**, 8673 (2003).
[34] I. M. Hodge and A. R. Berens, Macromolecules **15**, 762 (1982).
[35] I. M. Hodge and A. R. Berens, Macromolecules **20**, 2897 (1987).
[36] M. Schmidt, M. Olsson, and F. H. J. Maurer, J. Chem. Phys. **112**, 11 095 (2000).
[37] A. L. M. Smits, M. Wübbenhorst, P. H. Kruiskamp, J. J. G. van Soest, J. F. G. Vliegenthart, and J. van Turnhout, J. Phys. Chem. B **105**, 5630 (2001).
[38] O. E. Mogensen, *Positron Annihilation in Chemistry* (Springer-Verlag, Berlin, 1995).
[39] H. Sillescu, R. Böhmer, G. Diezemann, and G. Hinze, J. Non-Cryst. Solids **307**, 16 (2002).
[40] K. Vollmayr, W. Kob, and K. Binder, Europhys. Lett. **32**, 715 (1995).
[41] K. Vollmayr-Lee, W. Kob, K. Binder, and A. Zippelius, Int. J. Mod. Phys. C **10**, 1443 (1999).
[42] K. Vollmayr, W. Kob, and K. Binder, Phys. Rev. B **54**, 15 808 (1996).
[43] A. K. Doolittle, J. Appl. Phys. **22**, 1471 (1951).
[44] R. Wimberger-Friedl and J. G. de Bruin, Macromolecules **29**, 4992 (1996).
[45] C. G. Robertson and G. L. Wilkes, Macromolecules **33**, 3954 (2000).
[46] P. A. O'Connell and G. B. McKenna, Polym. Eng. Sci. **37**, 1485 (1997).